DYNAMIC FAILURE OF METALLIC CELLULAR MATERIALS

S. LEE and H.D. ESPINOSA
Department of Mechanical Engineering, Northwestern University, Evanston, IL 60208-3111, USA.

ABSTRACT

The quasi-static and dynamic compressive behavior of open-cell foams, textile cores, and pyramidal truss cores were investigated using a combination of experimental apparatus. Quasi-static tests were performed using a miniature loading stage and a Kolsky bar apparatus was used for intermediate deformation rates. For high deformation rates, a gas gun was employed. Optical observations of the sample deformation were performed in real time by means of high-speed photography. The deformation modes were investigated in detail from acquired images and digital image correlation. For the open cell foams, comparison between deformation fields under quasi-static and Kolsky bar loading revealed a moderate micro-inertia effect, where the inertia associated to the bending and buckling of ligaments delayed strain localization. Gas gun experiments performed on the same samples revealed a totally different deformation mode. A crashing shock wave was generated at the impact surface and propagated through the specimen. In these experiments both forward and reverse impact tests were performed to interrogate the state of stress in front and behind the shock wave front. Through these experiments, it was confirmed that the generation and propagation of shock waves within foam materials greatly enhance their energy absorption. For the case of textile cores, the mechanical response was found to be similar to the open cell foam materials. No significant difference in load-deformation histories and failure modes were observed between quasi-static and intermediate deformation rates. As in the case of open cell foams, at high deformation rates, the failure mode was governed by the development of a crushing shock wave. For the truss cores, significant deformation rate effects on peak stress and energy absorption were identified. Inertia effects appeared to dominate the core response because of two effects: i) the propagation of a plastic wave along the truss members, and ii) buckling induced lateral motion. In this article we provide a quantification of load-deformation response and associated failure modes across the sample as captured by high speed photography and image correlation.

1 INTRODUCTION

Materials combining light-weight and mechanical energy absorption are of primary interest in the protection design in automotive, locomotive, naval structures, and aerospace. Metallic cellular materials have been promising and attracting in many applications [1]. These materials offer low densities and are highly efficient in absorbing mechanical energy from external loading. Exploiting minimum weight design, material fabrication, structural integrity, dynamic experiments, and large-scale simulations, dramatic improvements can be made in the design of cellular materials exhibiting periodic cellular topologies.

Major contributions have been recently made in the mechanical characterization of foams materials at high rates of deformation. Reid and Peng [2] observed an increase of strength for higher deformation rates on cellular structures. On the other hand, Deshpande and Fleck [3] did not observe any rate dependency for the crashing stress of aluminum foams. These discrepancies from different experiments might be explained by failure and deformation mode transition such as the formation of shock waves within the specimen at very high strain rates. A model for shock waves in closed cell aluminum foams was proposed by Reid and co-workers [4]. It is shown in this model that the stress in the sample is not homogeneous and that therefore the measured stress is dependent on which end of the sample the data is recorded experimentally. Another potential source of rate dependency is micro-inertia which has been hypothesized and modeled but not directly observed on foam materials.

Previous studies on the behavior of cellular materials have been mainly performed on foam materials with randomly shaped and distributed cells. Newly proposed approaches utilize metallic core materials which are topologically-structured at small scale. Metallic woven textile materials were first developed by Sypeck and Wadley [5]. Theoretical and numerical analysis on the textile cores were performed and design optimization was pursued by Zok et al. [6]. Quasi-static compression, shear, and bending experiments were carried out on the textile cores by Mumm et al. [7]. Another new cellular material following similar manufacturing ideas is the so-called truss core. Truss cores with tetragonal and pyramidal topologies were theoretically studied by Wicks and Hutchinson [8]. They were predicted to offer the best combination of compressive strength and low weight. Experimental measurements and numerical simulations were performed to validate this prediction by Chiras et al. [9]. Whereas these truss cores were studied theoretically and numerically, limited experimental data was reported and the performed experiments were limited to quasi-static loading.

This article presents results from experiments on aluminum open cell foam, stainless steel textile core, and stainless steel pyramidal truss cores at three different deformation rates. Quasi-static tests were performed on a sub-miniature loading frame, intermediate strain rate tests were performed on a stored energy Kolsky bar, and high strain rate compression tests were performed using a light gas gun. In addition to compressive stress-strain curves at various strain rates, *real-time* observations were made in all tests by means of high speed digital imaging. Correlation techniques were used to reveal the mode of deformations and failure for the cellular materials. The results are compared for all the explored deformation rates. In addition, dynamic failure modes of textile and truss cores are reported as well as the measured load-deformation behaviors at different deformation rates.

2 ALUMINUM FOAM MATERIALS

2.1 Materials

The specimens were Duocel 6101-T6 Aluminium alloy foam with open cell architecture. The average cell size was 0.5 mm and the specimens had 7% relative density. The dimensions of the specimens were 25.4 mm × 17.78 mm × 17.78 mm.

2.2 Response at different deformation rates

Fig. 1 shows curves of nominal stress (F/A_0) versus nominal strain (δ/L_0) for quasi-static and dynamic compression tests on the Aluminum foam material. The deformation rates were 7×10^{-3} s^{-1} for the quasi-static case, ~250 s^{-1} for the Kolsky bar and 2500~3300 s^{-1} for the gas gun. The gas gun experiment was performed using the forward configuration, i.e., the specimen is attached to a transmission bar and it is impacted by a lunched bar. Details of the experimental set ups are given in [10]. Examination of the stress-strain lots reveals that the deformation rate seems to have no effect on the plateau stress of about 2.5 MPa throughout the explored strain rates. The densification occurs at a nominal strain of about 60%. The gas gun experiments show a stiffer densification response during the final crushing stages. This is connected to the arrival of the crashing front to the transmission bar as will be discussed later in the context of the formation of a crashing shock wave in the sample.

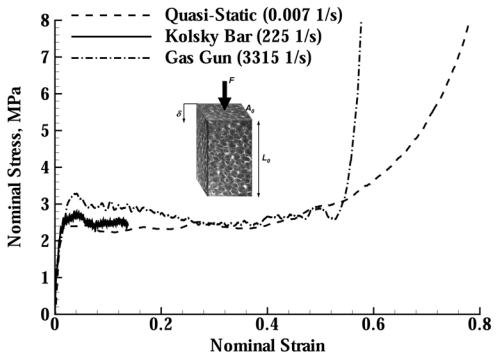

Figure 1: Stress-strain curves of compression of Al foam at different strain rates.

Although the deformation rate does not seem to have an effect on the overall compressive behavior, it seems to control the cells local deformation and failure modes. Fig. 2 shows snapshots of the specimen for quasi-static and Kolsky bar tests with superimposed x-direction strain fields obtained by digital image correlation. The images show that the overall nominal deformation in the dynamic case is more distributed than in the quasi-static case in which cell collapse is concentrated in one or two bands. The large deformations leading to cell crushing involve significant motion of material through bending and buckling of cell walls and ligaments. At high deformation rates, this motion results in a micro-inertia effect, and the result is that it takes more force and time to crush the cells. This phenomenon did not manifested itself in an appreciable increase in nominal crashing stress but the DIC analysis clearly shows that at intermediate strain rates the specimen seems to offer more resistance to strain localization. Fig. 3 shows a failure mode comparison between quasi-static and gas gun experiments. The stress was measured in the back side of the sample (forward impact configuration). As observed in the images, a major change in failure mode occurs with the development of a shock wave at high enough strain rates. The foam collapse produces a shock front perpendicular to the loading axis. This front propagates along the impact direction with a specific velocity [10]. In order to measure the stress behind the crushing shock front, a reverse impact experiment was performed.

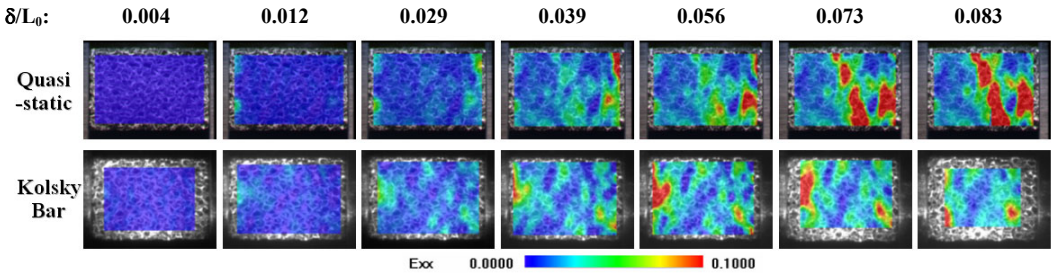

Figure 2: Differences in local deformations during quasi-static and Kolsky bar experiments.

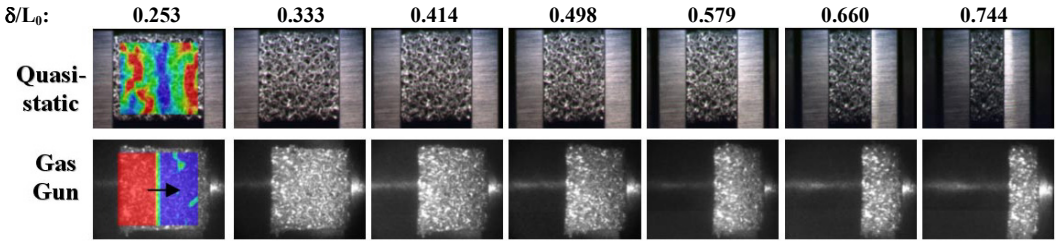

Figure 3: Different failure modes of deformations in comparison of quasi-static and gas gun experiments.

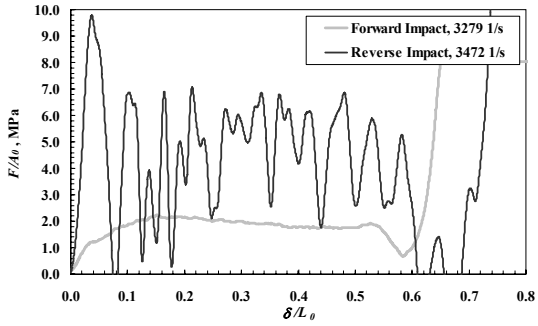

Figure 4: Comparison between reverse and forward impact test results in gas gun experiments.

2.3 Reverse impact experiments

In a reverse impact test, the specimen is launched with the striking bar. As a result, the transmitter bar records the loads behind the shock front initiated from the impact surface. It implies that the reverse impact test measures the crushing load while the forward impact test measures the load transmitted through the core. A comparison between forward and reverse impact results is shown in the Fig. 4. The average of load measured

in reverse impact is higher than that of the forward impact and consistent with theoretical predictions [4, 10]. Considering the fact that these two tests were carried out at almost the same strain rate, it can be concluded that the crushing load is higher than the load transmitted through the foam at high speeds of deformation. The fluctuations in the reverse impact test seem to be the result of local instabilities of cells clusters within the foam.

3 WOVEN TEXTILE CORE MATERIALS

3.1 Specimens

Stainless steel 304 woven textile core materials were fabricated at University of Virginia. The relative density of the core was 12.6%. SS 304 wires of 0.508 mm diameter were woven into a layer which has diamond-shaped cells. The average cell size was 3.24 mm × 3.24 mm along the wires. The woven layers were stacked into 15.45 mm thickness. The thickness of the textile core in the loading direction was 17.63 mm and the width was 18.55 mm.

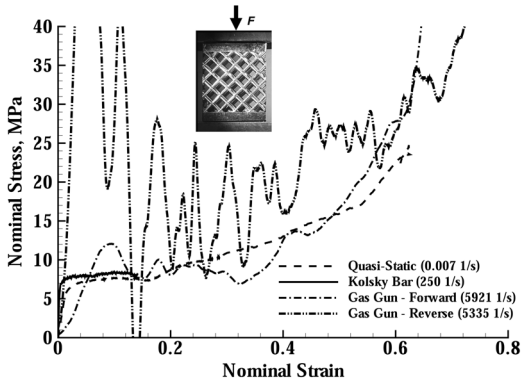

Figure 5: Stress-strain curves of compression of textile cores at different strain rates.

3.2 Response at different deformation rates

The stainless steel 304 woven textile core specimens were compressed at different regimes of deformation rates. In quasi-static loading, the relative velocity between two compression platens was 1×10^{-4} m/s, corresponding to a strain rate of 7×10^{-4} s^{-1}. The dynamic experiments were performed at a relative velocity of 4~6 m/s (deformation rate of 230~330 s^{-1}) in the Kolsky bar apparatus, while deformation velocities in the range of 72~104 m/s (deformation rate of 4129~5921 s^{-1}) were achieved in the gas gun set-up. Curves of load versus relative deformation of textile cores under

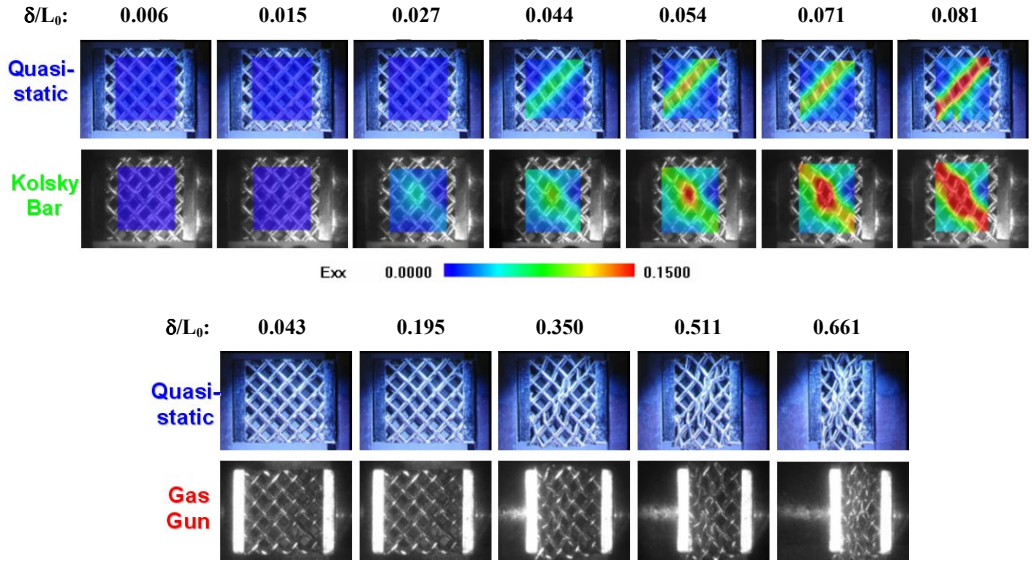

Figure 6: Failure sequences of woven textile cores at different strain rates.

different loading rates are given in Fig. 5. The curves show minor difference across the explored deformation rates. The load reaches a peak value after an initial elastic region and thereafter is almost constant, which can be considered as a plateau. The specimen behavior exhibits a progressive densification with an associated monotonic increase in stress. The peak stress appears to increase slightly with the increase in deformation rate, but the area under the force-deformation curve is much less sensitive to the loading rate. The rate insensitivity of the textile cores to the force-deformation response is similar to the one observed in the investigated Al foam.

On the other hand, the failure mode has a well defined transition from quasi-static and Kolsky bar to gas gun where the shock wave formation is also observed. In gas gun tests, diamond-shaped cells adjacent to the impact surface collapsed first as shown in Fig. 6. A crushing front, parallel to the front face sheet, propagates through the core. This crushing front is associated to a shock front corresponding to a jump in stress and density. To measure the shock wave effect, reverse impact tests were carried out on the textile cores. Fig. 5 shows a comparison between forward and reverse impact results. Because brazing materials joining the core and the face sheet remained in gaps between ligaments in the reverse test, the initial peak load was determined by this extra mass and associated inertia effect. The shock wave effect is clearly observed after the initial spurious peak. While this stress is higher than one measured in the forward impact tests the evolution is similar. Again, the signal has many peak and valleys that can be correlated to multiple instabilities in the core.

4 TRUSS CORE MATERIALS

4.1 Materials

The sandwich panels with pyramidal truss core made of stainless steel 304 were fabricated at the University of California at Santa Barbara. The tested specimens had a relative density of 3.5% and a 4-sided pyramid structure. The core thickness was 11.65 mm and the span of one cell: 16.82 $\times$15.39 mm^2. Truss members had a width of 1.18 mm and a thickness of 1.18 mm. The face sheet thickness is 2.2 mm. This unit cell repeated over the whole panel in x- and y-directions so that it is representative of the truss core materials. The unit cell specimens were cut from the sandwich panel and extra materials were left at the joints to maintain the periodicity by strong enough joints.

4.2 Response at different deformation rates

Uniform compression tests were performed on unit cell specimens. In quasi-static loading, the relative velocity between face sheets was 8×10^{-5} m/s, corresponding to a strain rate of 7×10^{-3} s^{-1}. The dynamic experiments in the Kolsky bar were performed at a relative velocity of 2.5~6.4 m/s, which corresponds to a strain rate of 263~550 s^{-1}. In the gas gun, deformation velocities of 84.5~115 m/s were reached resulting in a nominal strain rate of about 7257~9875 s^{-1}. Fig. 7 shows plots of load versus relative displacement under quasi-static and dynamic loading. In all cases, after an initial nominal stress increase, the load reaches a peak value and then drops. This load-displacement behavior is characteristic of structures exhibiting instability. The buckling instability was observed with high speed photography. Inspection of Fig. 7 reveals that the peak load attained in the gas gun is the highest followed by the peak load measured in the Kolsky bar experiments. As expected from a theoretical view point, the peak load measured in the quasi-static experiments is the lowest. In terms

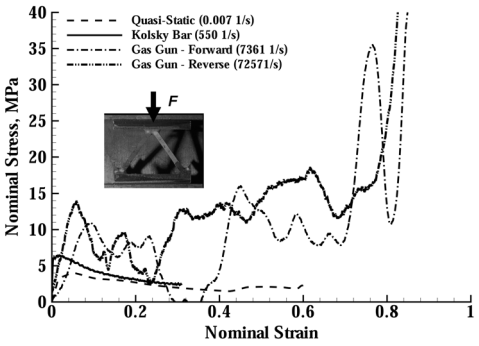

Figure 7: Stress-strain curves of pyramidal truss core being crushed at different strain rates.

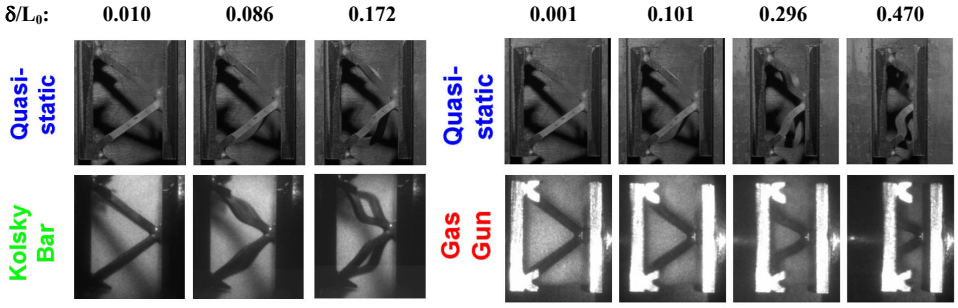

Figure 8: Failure sequences of pyramidal truss cores at different strain rates.

of nominal stress, the quasi-static peak stress is 4.0~4.2 MPa, almost half of the peak load in Kolsky bar loading (6.4 MPa). In the gas gun case, the peak stress is about 9.6~12.0 MPa. Additionally, comparison of areas under load-deformation responses shows that energy absorption up to a strain of 0.5 is a strong function of loading rate. In the gas gun experiments the dissipated energy is twice that of that in the quasi-static and Kolsky bar experiments. Again, the difference between quasi-static and 500 s^{-1} is modest. Both curves have the same features indicative of similar deformation behavior. High speed images later presented are consistent with this interpretation.

In the quasi-static and Kolsky bar experiments, the post-peak load smoothly decreases to what seems to be a steady state value, which is similar in both loading rates. On the other hand, several instabilities at different displacement levels are seen in the gas gun loading. Moreover, it is observed that the location of the multiple peaks in load is a function of the specimens as inferred from comparison of two experiments conducted at almost identical strain rate.

Examination of high speed images, Fig. 8, reveals a failure mode transition between the nominal strain rate imparted in the Kolsky bar and gas gun experiments. Careful inspection of the deformation in the truss members reveals that the buckling modes are dependent on the initial member imperfections. In some cases anti-symmetric mode of buckling is observed.

5 CONCLUSION

The compressive behavior of open cell aluminum foam, a textile stainless steel core and a pyramidal truss core was investigated, under various strain rates, using a unique combination of experiments. For the case of open cell foams, comparison between quasi-static and Kolsky bar experiments revealed moderate micro-inertia phenomena, where the inertia due to bending and buckling of the ligaments in the foam resisted strain localization. The gas gun experiments revealed a totally different deformation mode. A shock wave consisting of crashed material was generated at the impact surface and propagated through the specimen with a well defined speed. By performing gas gun experiments in forward and reverse configurations the stress level in front and behind the plastic or crushing shock front was measured. When the quasi-static, Kolsky bar and direct gas gun experiments are compared, the plateau or crashing stress is almost insensitive to strain rate. For the high strain rate experiments, this stress corresponds to the stress level in front of the propagating shock. We have also shown that generation and propagation of shock waves within foam materials greatly enhances their energy absorption. In light of this finding, foam materials should be tailored so that plastic shock waves are triggered in the applications of interest.

In the case of textile cores, the findings were quite similar to the ones observed in open cell foams. A well define failure mode transition was observed when the deformation rate was transitioned from 500 s^{-1} to 1×10^{4} s^{-1}. In the case of pyramidal truss core specimens significant strain rate effects on peak stress and energy absorption were observed. Micro inertia appears as the dominant effect in determining the peak nominal stress. A coupling between plastic wave

propagation (control by axial inertia) and buckling (lateral displacement) was observed. A very unique deformation of the members, at strain rates in the order of 1×10^4 s^{-1}, arises from deformation compatibility. Members are crash against the fast moving face sheet and make contact early on in the crashing process. The experiments also reveal that overall nominal stress – nominal strain curve is highly dependent on the initial imperfection of the members.

Further study should investigate the effect of the relative density on the peak stress and energy absorption of the material. The results could then be utilized to determine *optimal core* designs as a function of the application.

6 ACKNOWLEDGEMENTS

The authors would like to acknowledge F. Barthelat and N. Moldovan for their assistance in conducting the experiments. Special thanks are due to Professor J.W. Hutchinson from Harvard University and Professors A.G. Evans and F. Zok, and Dr. H. Rathbun from University of California at Santa Barbara for insightful discussions during the investigation reported here. The authors are also in debt to Professor H. Wadley and Drs. K. Dharmasena and D.T. Queheillalt from University of Virginia for their aid in the fabrication of samples and helpful discussions. This work was sponsored by the Office of Naval Research under Award No. 123163-02-N00014-02-1-0700.

7 REFERENCES

[1] Gibson, L.J. and Ashby, M.F., "Cellular Solids, Structure and Properties," 2nd ed., Cambridge University Press, Cambridge, UK, 1997.

[2] Reid, S.R. and Peng, C., "Dynamic Uniaxial Crushing of Wood," International Journal of Impact Engineering, Vol. 19, pp. 531-570, 1997.

[3] Deshpande, V.S. and Fleck, N.A., "High Strain Rate Compressive Behavior of Aluminium Alloy Foams," International Journal of Impact Engineering, Vol. 24, pp. 277-298, 2000.

[4] Harrigan, J.J., Reid, S.R., and Peng, C., "Inertia Effects in Impact Energy Absorbing Materials and Structures," International Journal of Impact Engineering, Vol. 22, No. 9-10, pp. 955-979, 1999.

[5] Sypeck, D.J. and Wadley, H.N.G., "Multifunctional Microtruss Laminates: Textile Synthesis and Properties," Journal of Materials Research, Vol. 16, No. 3, pp. 890-897, 2001.

[6] Zok, F.W., Rathbun, H.J., Wei, Z., and Evans, A.G., "Design of Metallic Textile Core Sandwich Panels," International Journal of Solids and Structures, Vol. 40, No. 21, pp. 5707-5722, 2003.

[7] Mumm, D. R., Wei, Z., Evans, A.G., Sypeck, D.J., and Wadley, H.N.G., "On the Performance of Light Weight Metallic Panels Fabricated Using Textile Cores," Submitted.

[8] Wicks, N. and Hutchinson, J.W., "Optimal Truss Plates," International Journal of Solids and Structures, Vol. 38, No. 30-31, pp. 5165-5183, 2001.

[9] Chiras, S., Mumm, D.R., Evans, A.G., Wicks, N., Hutchinson, J.W., Dharmasena, K., Wadley, H.N.G. and Fichter, S., "The Structural Performance of Near-Optimized Truss Core Panels," International Journal of Solids and Structures, 39 (15), pp. 4093-4115, 2002.

[10] Lee, S., Barthelat, F., Moldovan, N., Espinosa, H.D., and Wadley, H.N.G., "The Effects of Deformation Rates on Failure Modes of Open-Cell Al Foams and Textile Cellular Materials," Submitted to International Journal of Solids and Structures, 2004.